ANL-7646

Argonne National Laboratory

CALCULATIONS OF THE THERMODYNAMIC DRIVING FORCE FOR CARBON TRANSPORT IN SODIUM-STEEL SYSTEMS

by

K. Natesan and T. F. Kassner

The facilities of Argonne National Laboratory are owned by the United States Government. Under the terms of a contract (W-31-109-Eng-38) between the U. S. Atomic Energy Commission, Argonne Universities Association and The University of Chicago, the University employs the staff and operates the Laboratory in accordance with policies and programs formulated, approved and reviewed by the Association.

MEMBERS OF ARGONNE UNIVERSITIES ASSOCIATION

The University of Arizona
Carnegie-Mellon University
Case Western Reserve University
The University of Chicago
University of Cincinnati
Illinois Institute of Technology
University of Illinois
Indiana University
Iowa State University
The University of Iowa
Kansas State University
The University of Kansas
Loyola University
Marquette University
Michigan State University
The University of Michigan
University of Minnesota
University of Missouri
Northwestern University
University of Notre Dame
The Ohio State University
Ohio University
The Pennsylvania State University
Purdue University
Saint Louis University
Southern Illinois University
University of Texas
Washington University
Wayne State University
The University of Wisconsin

LEGAL NOTICE

This report was prepared as an account of Government sponsored work. Neither the United States, nor the Commission, nor any person acting on behalf of the Commission:

A. Makes any warranty or representation, expressed or implied, with respect to the accuracy, completeness, or usefulness of the information contained in this report, or that the use of any information, apparatus, method, or process disclosed in this report may not infringe privately owned rights; or

B. Assumes any liabilities with respect to the use of, or for damages resulting from the use of any information, apparatus, method, or process disclosed in this report.

As used in the above, "person acting on behalf of the Commission" includes any employee or contractor of the Commission, or employee of such contractor, to the extent that such employee or contractor of the Commission, or employee of such contractor prepares, disseminates, or provides access to, any information pursuant to his employment or contract with the Commission, or his employment with such contractor.

Printed in the United States of America
Available from
Clearinghouse for Federal Scientific and Technical Information
National Bureau of Standards, U. S. Department of Commerce
Springfield, Virginia 22151
Price: Printed Copy $3.00; Microfiche $0.65

ANL-7646
Metals, Ceramics,
and Materials

ARGONNE NATIONAL LABORATORY
9700 South Cass Avenue
Argonne, Illinois 60439

CALCULATIONS OF THE THERMODYNAMIC DRIVING FORCE FOR CARBON TRANSPORT IN SODIUM-STEEL SYSTEMS

by

K. Natesan and T. F. Kassner

Materials Science Division

December 1969

TABLE OF CONTENTS

	Page
ABSTRACT	7
I. INTRODUCTION	8
II. THERMODYNAMIC ASPECTS	9
A. Carbon Activity in Fe-Cr-Ni Alloys	9
B. Solubility of Carbon in Fe-Cr-Ni Alloys	11
C. Distribution of Carbon between Sodium and Fe-Cr-8 wt % Ni Alloys	11
D. Activity of Binary Carbides in Mixed Carbides	13
E. Compositional Changes during Carbide Precipitation	14
F. Carbon Solubility and Activity in Ferritic Steel	18
III. KINETIC ASPECTS	20
IV. EFFECT OF CARBURIZATION ON THE MECHANICAL PROPERTIES OF STAINLESS STEEL	22
V. CONCLUSIONS	22
APPENDIX	24
ACKNOWLEDGMENTS	26
REFERENCES	27

LIST OF FIGURES

No.	Title	Page
1.	Fe-C Phase Diagram	9
2.	The Effect of Chromium on the Carbon Activity in Fe-Cr-C Alloys at 1000°C	9
3.	Isoactivity Lines in the Fe-Cr-C System at 1000°C.	10
4.	A Plot of Carbon Activity at the γ-carbide Phase Boundary as a Function of Chromium Content in Fe-Cr-Ni Alloys	10
5.	Temperature Dependence of Carbon Activity at the γ-carbide Phase Boundary in Fe-Cr-8 wt % Ni Alloys for Various Chromium Levels in the Alloy	11
6.	Temperature Dependence of the γ-phase Field in Fe-Cr-8 wt % Ni Alloys	11
7.	Temperature Dependence of Carbon Solubility in the Fe-Cr-8 wt % Ni Alloys	12
8.	Temperature Dependence of Carbon Solubility in Sodium	12
9.	Temperature Dependence of Fe-Cr-8 wt % Ni Alloy (C sat)--$\underline{C}$(Na)--Carbide Equilibrium.	13
10.	A Schematic Diagram of the Change in Composition of the Austenite and Carbide during Carburization	15
11.	A Plot of Total Carbon Content in an Fe-18 wt % Cr-8 wt % Ni Alloy vs Carbon Concentration in Sodium at Different Temperatures	16
12.	A Plot of Total Carbon Content in an Fe-15 wt % Cr-8 wt % Ni Alloy vs Carbon Concentration in Sodium at Different Temperatures	16
13.	A Plot of Total Carbon Content in an Fe-12 wt % Cr-8 wt % Ni Alloy vs Carbon Concentration in Sodium at Different Temperatures	16
14.	A Schematic Diagram Relating Decarburization to Chromium Mass Transfer from an Alloy Exposed to Sodium	17
15.	The α-phase Field in Fe-2.25 wt % Cr-1 wt % Mo Steel as a Function of Temperature	19

LIST OF FIGURES

No.	Title	Page
16.	Temperature Dependence of Ferritic Steel and Austenitic Steel--C(Na)--Carbide Equilibria	20
17.	The Difference in the Concentration of Carbon between γ-Fe and Fe-8 wt % Ni Austenite as a Function of Carbon Activity in the Austenite at Temperatures of 800 and 1000°C	24
18.	The Difference in the Solubility of Carbon in a Fe-Cr Austenite and the Carbon Concentration in γ-Fe, per wt % Cr, at Iso-activity for Various Chromium Levels in the Fe-Cr-C Alloys	25

CALCULATIONS OF THE THERMODYNAMIC DRIVING FORCE FOR CARBON TRANSPORT IN SODIUM-STEEL SYSTEMS

by

K. Natesan and T. F. Kassner

ABSTRACT

The thermodynamic activity and solubility of carbon in Fe-Cr-Ni alloys were calculated in the temperature range 500-800°C by extrapolation of higher-temperature data in the Fe-Cr-C and Fe-Ni-C systems. The compositional range for the alloys included that of an 18-8 austenitic stainless steel. These results were used with phase-equilibria information and data for the solubility of carbon in sodium to obtain an equilibrium relationship between the total carbon content in the alloys (austenite carbon + carbide carbon) and carbon concentrations in sodium. The calculations showed that the Fe-Cr-Ni alloys with nominal initial carbon contents may undergo carburization or decarburization depending upon the carbon concentration in sodium and the temperature in the range 500-800°C. Computed carbon concentrations in sodium for incipient carbide formation in an 18-8 stainless steel are significantly lower (i.e., below 1 ppm) than carbon concentrations commonly reported (i.e., 15-30 ppm) for stainless steel-sodium systems operating at temperatures below 700°C.

The phase-equilibria and activity data were used to explain the observed phenomenon of transfer of carbon from austenitic steel to sodium when chromium depletion, due to mass transfer, occurs. In addition, the driving force for carbon transfer from ferritic to austenitic steel under isothermal conditions was calculated.

I. INTRODUCTION

Various types of stainless steel are being considered for use as structural and fuel-cladding materials in sodium-cooled fast breeder reactors. Ferritic steels with low chromium and molybdenum contents have been suggested for use in sodium-heated steam generators and intermediate heat exchangers. The major compatibility problems with these materials in a reactor system are: (1) the carburization-decarburization behavior of austenitic stainless steel exposed to the sodium environment, (2) corrosion and compositional changes resulting from mass-transfer processes involving the elements (e.g., Fe, Cr, Ni, and Mn) comprising the steel, and (3) decarburization of the ferritic steel resulting in a loss of strength of the steel.

The emphasis in this report is primarily on the carburization-decarburization phenomena and the carbon-transfer problem; subsequently, it will be shown that these areas are interrelated. Numerous experimental observations on carburization-decarburization behavior of both stainless and ferritic steel exposed to sodium have been reported; however, quantitative predictions based on these efforts have been difficult and uncertain. The problem is complicated by incomplete knowledge of the relative importance of the various carbon species present and of interactions between carbon and other nonmetallic impurities in liquid sodium. The carbon potential established by the same concentration of the various solute species (e.g., C, Na_2C_2 and NaCN) will be different, so that one species in sodium will be more carburizing to stainless steel than another.

Calculations, based upon thermodynamic data, have been made to determine the effect of variables such as carbon (graphite) concentration in sodium, temperature, and composition of iron-base alloys [e.g., Fe-12 to 18 wt % Cr-8 wt % Ni, and Fe-2.25 wt % Cr-1 wt % Mo (Croloy $2\frac{1}{4}$)] on carburization-decarburization phenomena. A relationship has been developed for the total carbon content of Fe-Cr-Ni alloys in equilibrium with specified carbon concentrations in sodium in the temperature range 500-800°C. The chromium concentration range from 12 to 18 wt % takes into account the effect of chromium depletion, due to mass transfer, from 18-8 stainless steel in sodium systems. The thermodynamics of carbon transfer between the ferritic and austenitic steel has also been explored over the temperature range 500-800°C.

In all the computations, carbon was considered as the major impurity in sodium and any interaction between carbon and other impurities (e.g., oxygen and nitrogen) was assumed negligible. At present, similar calculations for other carbon species in sodium are limited by the lack of accurate free-energy data in the case of Na_2C_2, and the absence of data on the interaction effect of nitrogen on the carbon activity coefficient in sodium containing NaCN. When these data become available, the relative carburizing potentials of these two species can be evaluated and compared with that of graphite by following the methods outlined in this report.

II. THERMODYNAMIC ASPECTS

A. Carbon Activity in Fe-Cr-Ni Alloys

Quantitative data in the literature on the activity and solubility of carbon in Fe-Cr-Ni alloys are scarce, in the temperature range of interest in sodium technology. An attempt is made in this report to calculate the thermodynamic activity and solubility of carbon in Fe-Cr-Ni alloys in the temperature range 500-800°C by extrapolating the available high-temperature data. For this purpose we started with the Fe-C binary system[1] (see Fig. 1), and then considered the effects of chromium and nickel on the binary carbon activity and solubility. The carbon solubility in metastable austenite at lower temperatures was obtained by extrapolating the γ-Fe_3C phase boundary below 723°C.

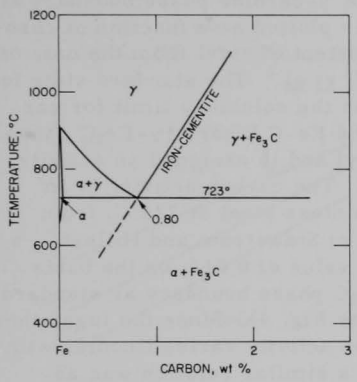

306-454 Rev. 1

Fig. 1. Fe-C Phase Diagram

Chromium is a carbide former that weakly interacts with iron and strongly reduces the carbon activity coefficient in austenite. Nickel is an austenite stabilizer that increases the activity coefficient of carbon in austenite, thereby resulting in a decrease in carbon solubility. The austenite in 18 wt % Cr-8 wt % Ni stainless steel is not thermodynamically stable, but the kinetics of the $\gamma \rightarrow \alpha +$ carbide transformation is negligibly slow so that, for all practical purposes, the 18-8 stainless steel may be considered as fully austenitic.

The effect of chromium on the activity of carbon in austenite at 1000°C was studied by Schenck and Kaiser[2] and by Bungardt et al.[3,4] The results of these investigations agree fairly well. Bungardt et al.[4] determined the activity of carbon at 1000°C in the Fe-Cr-C system, with chromium contents up to 9 wt % and carbon contents up to 4 wt %, by equilibrating the alloys with H_2-CH_4 gas mixtures. Their results are shown in Figs. 2

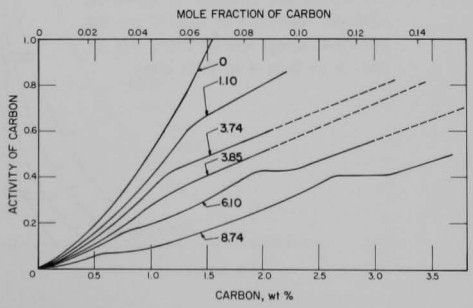

Fig. 2

The Effect of Chromium on the Carbon Activity in Fe-Cr-C Alloys at 1000°C.[4] The numbers on the curves indicate the wt % Cr in the alloys.

306-459 Rev. 1

and 3. Stawstrom and Hillert[5] made measurements of carbon activity in Type 304 stainless steel at 725°C by equilibrating the steel with a Fe-16 wt % Ni alloy in a partial vacuum of 150 Torr. They reported a carbon activity in the steel of about 0.01, with graphite as the standard state.

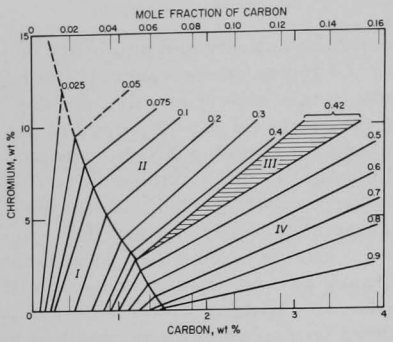

306-450 Rev. 1

Fig. 3. Isoactivity Lines in the Fe-Cr-C System at 1000°C.[4] The numbers on the lines indicate the carbon activity. I = γ phase, II = γ + $(Fe,Cr)_7C_3$, III = γ + $(Fe,Cr)_7C_3$ + $(Fe,Cr)_3C$, and IV = γ + $(Fe,Cr)_3C$.

In Fig. 4, the activity of carbon along the γ-carbide phase boundary at 1000°C is plotted as a function of chromium content of steel from the data of Bungardt et al.[4] The standard state for carbon is the solubility limit for carbon in the Fe-C binary (γ-Fe_3C phase boundary) and is assigned an activity of unity. The carbon activity in an 18-8 stainless steel at 725°C, from the data of Stawstrom and Hillert, yields a value of 0.014, on the basis of γ-Fe_3C phase boundary as standard state (see Fig. 4). Since the logarithm of carbon activity varies linearly with the chromium content of the alloy at 1000°C, a similar relation was assumed at 725°C. The effect of 8 wt % Ni on the carbon activity in Fe-Cr-C alloys at 1000°C (see Fig. 4) is negligibly small for the chromium range 12-18 wt %, as may be calculated from the data in the Appendix. Therefore, the results in Fig. 4 were used to obtain a semilogarithmic plot of carbon

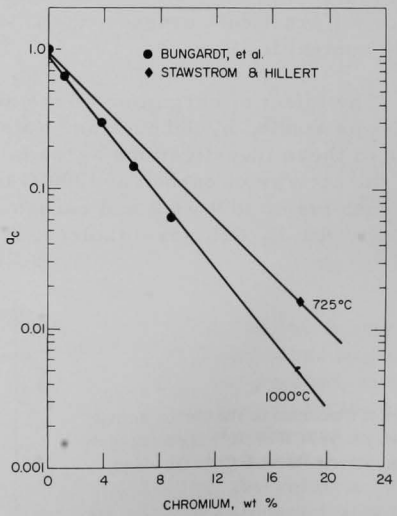

Fig. 4

A Plot of Carbon Activity at the γ-carbide Phase Boundary as a Function of Chromium Content in Fe-Cr-Ni Alloys. The data at 1000°C are for Fe-Cr-C alloys and at 725°C for an Fe-18 wt % Cr-8 wt % Ni alloy.

306-455 Rev. 1

activity in Fe-Cr-8 wt % Ni alloys versus reciprocal temperature (see Fig. 5). This figure can be used to obtain the carbon activity values at lower temperatures.

B. Solubility of Carbon in Fe-Cr-Ni Alloys

The carbon solubility values in Fe-Cr-8 wt % Ni alloys at different temperatures were computed, in the manner described in the Appendix, by applying the interaction effect of nickel and chromium on the solubility of carbon in Fe-C austenite. These calculations were made using the Fe-Ni-C data of Heckler and Winchell,[6] the Fe-Cr-C data of Bungardt et al.,[4] and the results of Rocha's[7] sensitization studies on 18-8 stainless steel. Figure 6 shows the carbon solubilities (γ-phase boundary), as a function of chromium concentration, in Fe-Cr-8 wt % Ni alloys at different temperatures. A semilogarithmic plot of carbon solubility versus reciprocal temperature for alloys with chromium levels of 12, 15, and 18 wt % is shown in Fig. 7.

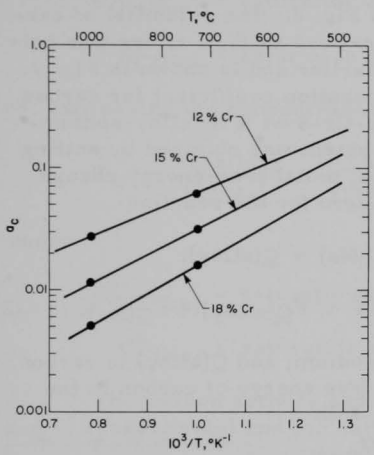

306-451 Rev. 1

Fig. 5. Temperature Dependence of Carbon Activity at the γ-carbide Phase Boundary in Fe-Cr-8 wt % Ni Alloys for Various Chromium Levels in the Alloy

C. Distribution of Carbon between Sodium and Fe-Cr-8 wt % Ni Alloys

The distribution coefficient, which is the equilibrium ratio of carbon concentration in an Fe-Cr-Ni alloy to the carbon concentration in sodium, was derived by equating the partial molal free energies of carbon in the alloy and the sodium. The calculations made here are based on the thermodynamic treatment of the partitioning of oxygen between refractory metal and sodium discussed by Kassner and Smith.[8]

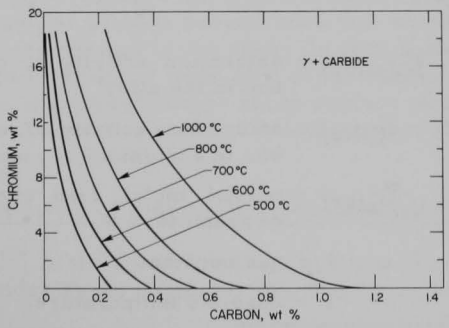

Fig. 6
Temperature Dependence of the γ-phase Field in Fe-Cr-8 wt % Ni Alloys

306-458 Rev. 1

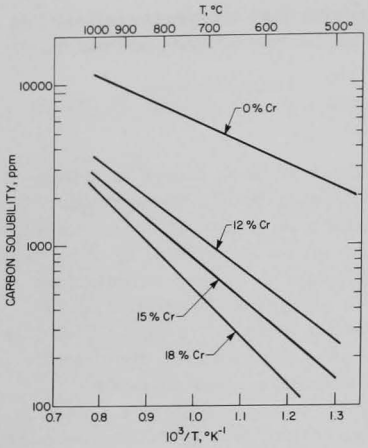

306-457 Rev. 1

Fig. 7. Temperature Dependence of Carbon Solubility in the Fe-Cr-8 wt % Ni Alloys

The temperature dependence of the solubility of carbon in liquid sodium was evaluated from the results of Longson and Thorley:[9]

$$\underline{C}(\text{ppm})^* = 5.03 \times 10^7 \exp(-13740/T). \quad (1)$$

The solubility of carbon in sodium, as a function of reciprocal temperature, is shown in Fig. 8. The solubility of carbon in Fe-Cr-8 wt % Ni alloys was calculated earlier and is shown in Fig. 7. The distribution coefficient for carbon in the Fe-Cr-8 wt % Ni alloy-sodium-carbon system was obtained by setting the partial molal free-energy change equal to zero for the reaction

$$\underline{C}(\text{Na}) = \underline{C}(\text{alloy});$$

$$\Delta F = \overline{F}_{\underline{C}}(\text{alloy}) - \overline{F}_{\underline{C}}(\text{Na}), \quad (2)$$

where $\underline{C}(\text{Na})$ denotes carbon in solution in sodium, and $\underline{C}(\text{alloy})$ is carbon in solution in the alloy. The partial molal free energy of carbon in the alloy at the γ-carbide phase boundary with graphite as the standard state is given by

$$\overline{F}_{\underline{C}}(\text{alloy}) = RT \ln a_{\underline{C}}(\text{alloy}). \quad (3)$$

Following the formalism of Kassner and Smith,[8] the result is

$$\frac{a_{\underline{C}}(\text{alloy})}{a_{\underline{C}}(\text{Na})} = \frac{a^0_{\underline{C}}(\text{alloy})}{a^0_{\underline{C}}(\text{Na})} \exp\left\{\frac{\overline{F}_{\underline{C}}(\text{gr}) - \overline{F}_{\underline{C}}(\text{alloy})}{RT}\right\}, \quad (4)$$

where

$a^0_{\underline{C}}(\text{alloy})$ = saturation activity of carbon in the alloy

$a^0_{\underline{C}}(\text{Na})$ = saturation activity of carbon in sodium

$\overline{F}_{\underline{C}}(\text{gr})$ = partial molal free energy of graphite = 0

R = gas constant

T = absolute temperature.

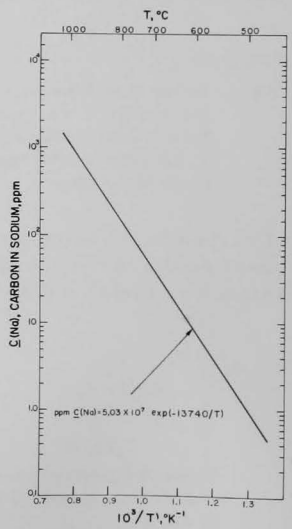

306-456 Rev. 1

Fig. 8. Temperature Dependence of Carbon Solubility in Sodium[9]

*ppm designates parts per million by weight.

If the carbon in the alloy and the sodium obeys Henry's law ($a_{\underline{C}} = kN_{\underline{C}}$), the distribution coefficient in terms of atom fraction of carbon is

$$K_A = \frac{N_{\underline{C}}(\text{alloy})}{N_{\underline{C}}(\text{Na})} = \frac{N^0_{\underline{C}}(\text{alloy})}{N^0_{\underline{C}}(\text{Na})} \exp\left\{\frac{-\overline{F}_{\underline{C}}(\text{alloy})}{RT}\right\}, \tag{5}$$

where

$N^0_{\underline{C}}(\text{alloy})$ = saturation atom fraction of carbon in the alloy

$N^0_{\underline{C}}(\text{Na})$ = saturation atom fraction of carbon in sodium;

or, expressing the concentrations in ppm, we obtain

$$K_W = \frac{C_{\underline{C}}(\text{alloy})}{C_{\underline{C}}(\text{Na})} = \frac{C^0_{\underline{C}}(\text{alloy})}{C^0_{\underline{C}}(\text{Na})} \exp\left\{\frac{-\overline{F}_{\underline{C}}(\text{alloy})}{RT}\right\}, \tag{6}$$

where

$C^0_{\underline{C}}(\text{alloy})$ = saturation concentration of carbon in the alloy, ppm

$C^0_{\underline{C}}(\text{Na})$ = saturation concentration of carbon in sodium, ppm.

The carbon activity and solubility data for the alloys (see Figs. 5 and 7, respectively) and the carbon solubility values for sodium (see Fig. 8) were used with Eq. 6 to evaluate the carburizing potential of carbon in sodium at different temperatures, which is shown in Fig. 9. It is evident from this figure that sodium containing more than 0.65 ppm carbon will lead to precipitation of $(Cr,Fe)_{23}C_6$ carbide in Fe-18 wt % Cr-8 wt % Ni alloy at 700°C.

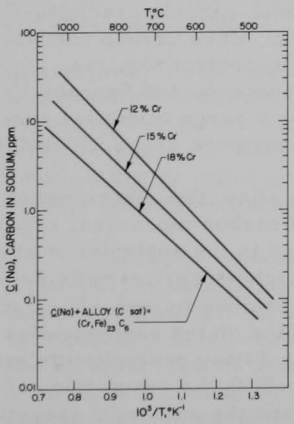

306-460 Rev. 1

Fig. 9. Temperature Dependence of Fe-Cr-8 wt % Ni Alloy (C sat)--$\underline{C}$(Na)--Carbide Equilibrium

On the other hand, if depletion of chromium occurs at the surface of the steel due to the dissolution processes, then, with 0.65 ppm carbon in sodium, no carbide precipitation will be observed near the surface in the alloy. In fact, if the chromium level drops to 12 wt % at the surface of the alloy, then precipitation at the surface is expected only if carbon in solution in sodium exceeds 2.6 ppm at 700°C.

D. Activity of Binary Carbides in Mixed Carbides

In the Fe-C and Cr-C systems, the binary carbides Fe_3C, $Cr_{23}C_6$, Cr_7C_3, and Cr_3C_2 have been

reported. As a result of the intersolubility of the binary carbides in the Fe-Cr-C system, the corresponding mixed carbides $(Fe,Cr)_3C$ with up to 15 wt % chromium, $(Cr,Fe)_{23}C_6$ with up to 30 wt % iron, and $(Cr,Fe)_7C_3$ with up to 60 wt % iron are formed.[10] On the assumption that the free energy of mixing in the mixed carbides is due entirely to the entropy of mixing of metallic atoms with no contribution due to carbon and no heat of mixing, Richardson[11] has shown that there should be a power relationship between the activity and mole fraction of Mn_3C in the mixed carbide $(Fe,Mn)_3C$. The ideal mixing model has been successfully applied by Butler et al.[12] to $(Fe,Mn)_7C_3$ carbide, and they have shown very good agreement of the experimental data with the model. The model may be applied to solid solutions of carbides in which the metal atoms are similar in size and properties. The behavior of chromium is probably similar to that of manganese in mixed carbides, since Fe, Cr, and Mn are similar in structure and properties. Therefore, the model was applied to $(Cr,Fe)_{23}C_6$ carbide in our calculations.

E. Compositional Changes during Carbide Precipitation

In any Fe-Cr-8 wt % Ni alloy, a solubility limit for carbon exists at different temperatures, as shown in Fig. 7. If the solubility limit for carbon is exceeded because of the carbon potential in sodium, then precipitation of a second phase [e.g., $(Cr,Fe)_{23}C_6$, $(Cr,Fe)_7C_3$, or $(Fe,Cr)_3C$] occurs, depending on the temperature and chromium content of the alloy and on the carburizing potential in sodium. For the range of chromium levels in the alloy between 10 and 20 wt % and for the temperature range 500-800°C, the $(Cr,Fe)_{23}C_6$ carbide is expected. Such carbide precipitation was reported by Bogers and Chirer[13] and Hiltz[14] when carbon concentrations in the sodium were low. At high carbon concentrations, the $(Cr,Fe)_7C_3$ carbide was reported by Hiltz and by Anderson and Sneesby.[15] The calculations in this report were made only for a range of carbon contents for which $(Cr,Fe)_{23}C_6$ is expected in the temperature range 500-800°C.

For a given chromium concentration in an alloy, the concentration of chromium in austenite decreases, while that of carbon increases, as the carbide is precipitated. This compositional change in the austenite is accompanied by the precipitation of carbide with a higher (Fe/Cr) ratio so that the larger the carburization, the richer the carbides in iron. Such an observation was reported by Valibus[16] during studies on the carburization of steels in sodium. These compositional changes during precipitation are indicated schematically by the arrows in Fig. 10. With the assumption of local equilibrium between the precipitated phase and the austenite, isoactivity lines similar to those in Fig. 10 were constructed at different temperatures from the reaction

$$\tfrac{23}{6}\,Cr(\gamma) + C(\gamma) = \tfrac{1}{6}\,Cr_{23}C_6 \text{ (in mixed carbide).} \qquad (7)$$

The equilibrium constant K for Reaction 7 is

$$K = \frac{a_{Cr_{23}C_6}^{1/6}}{a_{C(\gamma)} a_{Cr(\gamma)}^{23/6}}. \tag{8}$$

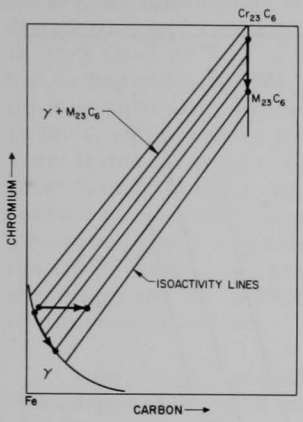

308-2091 Rev. 1

Fig. 10

A Schematic Diagram of the Change in Composition of the Austenite and the Carbide during Carburization

The free-energy change for Reaction 7, as a function of temperature, is given[11] by

$$\Delta F^{\circ}_{298-1673^{\circ}K} = -16{,}380 - 1.54T. \tag{9}$$

The measurement of activities in the Fe-Cr binary system at 1200°C by McCabe et al.[17] showed that chromium exhibited a slight positive deviation from the Raoult's-law line. On the other hand, the chromium activity measurements made by Jeannin et al.,[18] in the temperature range 1040-1300°C, indicated substantial positive deviation from the Raoult's-law line. Therefore, with or without justification, as a first approximation γ_{Cr} was assigned a value of unity in our calculations of isoactivity lines at 500, 600, 700, and 800°C.

For any chromium content in the alloy, these tie lines will establish a relation between the total carbon content (carbon in austenite + carbon in carbide) and the carbon concentration in austenite. From the above relationship, and the relation between carbon in austenite and carbon in sodium (see Fig. 9), a dependence of the total carbon on the carbon concentration in sodium was obtained for various chromium levels in the alloy at different temperatures. Figures 11-13 show this relationship at different temperatures for Fe-Cr-8 wt % Ni alloys with 18, 15, and 12 wt % chromium in the alloy, respectively.

Figure 11 indicates that if an 18-8 stainless steel is exposed to liquid sodium containing about 2 ppm carbon in solution at 700°C, the surface will exhibit a total carbon concentration of about 0.59 wt %. The surface concentration probably is established in a short time compared with the duration of most experiments. If the specimen is exposed to the sodium for a sufficient time, the entire specimen will attain a uniform total carbon concentration of 0.59 wt %. A decrease in temperature for the same carbon concentration in sodium will result in a much larger surface and uniform carbon concentration in the alloy upon equilibration, as can be seen from Fig. 11. The alloy at lower temperatures will obviously take a much longer time to reach the final equilibrium state. An attempt is made in a later section to examine the kinetics of the process.

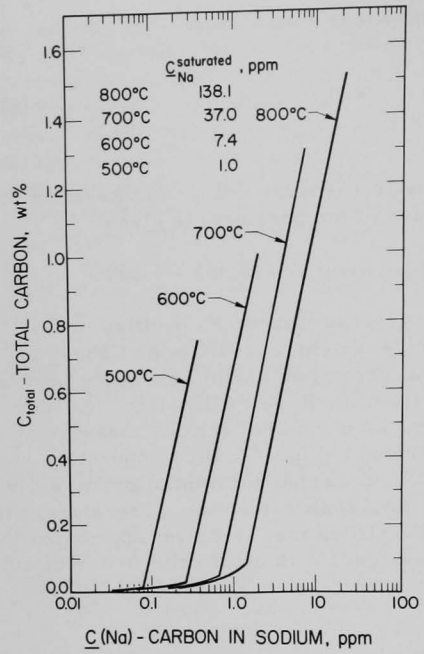

306-465 Rev. 2

Fig. 11. A Plot of Total Carbon Content in an Fe-18 wt % Cr-8 wt % Ni Alloy vs Carbon Concentration in Sodium at Different Temperatures. The carbide contribution to the total carbon in these curves is from the $M_{23}C_6$ type.

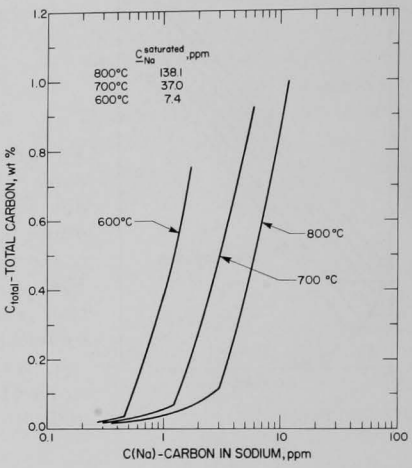

306-464 Rev. 2

Fig. 12. A Plot of Total Carbon Content in an Fe-15 wt % Cr-8 wt % Ni Alloy vs Carbon Concentration in Sodium at Different Temperatures. The carbide contribution to the total carbon in these curves is from the $M_{23}C_6$ type.

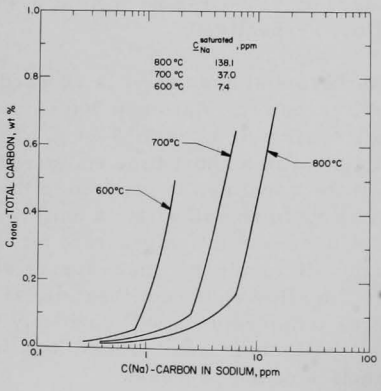

Fig. 13

A Plot of Total Carbon Content in an Fe-12 wt % Cr-8 wt % Ni Alloy vs Carbon Concentration in Sodium at Different Temperatures. The carbide contribution to the total carbon in these curves is from the $M_{23}C_6$ type.

306-461 Rev. 2

A number of investigators[19,20] have reported that, in corrosion tests, the chromium concentration at the surface of Types 316 and 304 stainless steel decreases upon exposure to flowing sodium. Surface concentrations for chromium as low as 8 wt % have been determined for Type 316 stainless steel and 15 wt % for Type 304 stainless steel following a 2000-hr exposure to flowing sodium at 705°C.[20] The calculations suggest observable differences in the carbon concentration profile and the carbide distribution within the diffusion zone during the carburization of an Fe-18 wt % Cr-8 wt % Ni alloy, depending upon whether chromium depletion had or had not occurred. For example, Fig. 11 shows that an Fe-18 wt % Cr-8 wt % Ni alloy exposed to sodium containing 2 ppm carbon in solution at 700°C will result in a surface carbon concentration of 0.59 wt %. However, if the chromium concentration near the surface was depleted to 12 wt % and the alloy exposed to sodium under the same conditions, the surface carbon concentration will be 0.08 wt % (see Fig. 13) with no carbide precipitate. Even though no precipitate is expected at the surface of the alloy, carbide can precipitate within the alloy at a depth where the chromium and the carbon concentrations are sufficient for the γ-carbide equilibrium to prevail.

Roy et al.[20] reported that Type 304 stainless steel decarburized when exposed to liquid sodium at 705°C, and the process was accompanied by chromium depletion. The observed phenomenon of chromium depletion accompanied by carbon transfer from the alloy to sodium may be examined by using Fig. 14. In this figure χ^i_{Cr} and χ^i_C represent the initial concentrations of chromium and carbon in the alloy. It may be noted that the total carbon in the alloy is higher than the solubility limit for carbon in the alloy. Let us assume, for simplicity, that the carbon activity in sodium is the value required to yield a total carbon concentration of χ^i_C in the alloy. In a large sodium system, the carbon concentration and activity in the sodium will change very little as the alloy becomes depleted in carbon to a final value χ^f_C. Consequently, the final carbon concentration in the alloy χ^f_C will be established by an isoactivity line, as shown in Fig. 14. As the chromium concentration in the alloy decreases because of corrosion mass-transfer, decarburization to a new equilibrium carbon level in the alloy will occur.

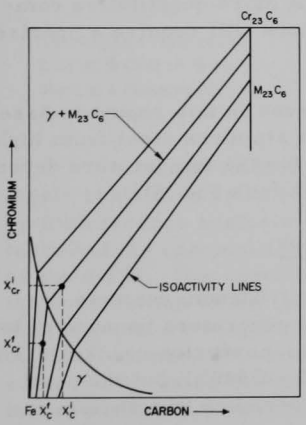

Fig. 14. A Schematic Diagram Relating Decarburization to Chromium Mass Transfer from an Alloy Exposed to Sodium

Quantitatively, Type 304 stainless steel initially has about 0.07 wt % carbon and 18 wt % chromium (i.e., χ^i_{Cr} = 18.0 wt %; χ^i_C = 0.07 wt %). At 705°C, a carbon concentration of 0.68 ppm in sodium (see Fig. 11) will yield

a total carbon value of 0.07 wt % in the alloy. If the alloy lost chromium such that χ^f_{Cr} = 15.0 wt %, then the carbon content in equilibrium with the alloy may be calculated by using the distribution coefficient for 15 wt % chromium alloy at 705°C. The distribution coefficient K_W at 705°C can be computed by using Figs. 7 and 9:

$$K_W \text{ (for 15 wt \% Cr alloy)} = \frac{730}{1.4} = 520.$$

Therefore,

$$\chi^f_C = K_W \times \underline{C}(Na) = 520 \times 0.68$$

$$= 354 \text{ ppm} \simeq 0.035 \text{ wt \%}.$$

Similarly, if the chromium in the alloy decreased to 12 wt % (χ^f_{Cr} = 12 wt %), then

$$\chi^f_C = \frac{1100}{2.8} \times 0.68 = 268 \text{ ppm} \simeq 0.027 \text{ wt \%}.$$

Thus, the observed phenomenon can be explained provided the carbon activity in the sodium is low but not sufficiently low to produce carbon transfer in the absence of chromium depletion. A more quantitative comparison between observations and these calculations will require a precise analysis of the carbon concentration in sodium.

At present it is not prudent to use the curves in this report to assess the driving force for athermal carbon transfer in stainless steel from high to low temperatures because of the meager data for the temperature dependence of the carbon activity in the Fe-Cr-Ni alloys (see Fig. 5).

F. Carbon Solubility and Activity in Ferritic Steel

Ferritic steels with low chromium and molybdenum contents are being considered for use in sodium-heated steam generators because of low cost and lack of susceptibility to water-side stress-corrosion cracking. This type of steel was found to be satisfactory up to about 540°C, but the steel decarburized at a significant rate above this temperature in a sodium environment.[21] An Fe-2.25 wt % Cr-1 wt % Mo steel section from sodium-loop piping that had operated at 590°C for 20,000 hr was found to be almost completely decarburized. The carbon content of the piping decreased from the initial value of 0.105 to about 0.025 wt %. The decarburization causes the material to lose tensile strength and reduces its stress-rupture life. Furthermore, the carbon transferred to the sodium can carburize any high-temperature austenitic stainless steel that is used in the system,

with a resultant loss in ductility of the stainless steel. The rate of decarburization depends on the temperature as well as upon the carbon activity in the steel and in sodium.

The thermodynamic activity of carbon, as a function of carbon content in an Fe-2.25 wt % Cr-1 wt % Mo steel, was calculated starting from the αFe-C binary system and considering the interaction effect of molybdenum and chromium on carbon. The cementite solubility curve in the αFe-C binary, from the work of Smith,[22] is shown in Fig. 15.

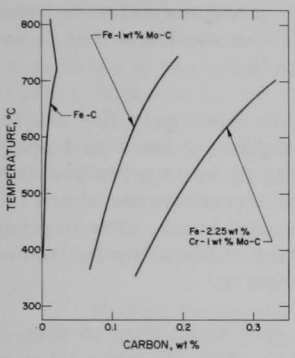

306-463 Rev. 1

Fig. 15

The α-phase Field in Fe-2.25 wt % Cr-1 wt % Mo Steel as a Function of Temperature

Molybdenum is a ferrite stabilizer that, at constant carbon activity, decreases the activity coefficient for carbon and thereby results in an increase in concentration of carbon in αFe. The effect of 1 wt % molybdenum on the solubility of carbon in αFe[1] is also shown in Fig. 15. The effect of chromium on the activity coefficient of carbon in αFe was studied by Petrova et al.[23] They determined the chromium-carbon interaction parameter in αFe, $f_C^{(Cr)} = 0.50$. This parameter was found to be almost temperature insensitive. By using this parameter, the solubility of carbon in Fe-2.25 wt % Cr-1 wt % Mo alloy was calculated, and the result is shown in Fig. 15. The calculation showed that at 700°C the above alloy can dissolve up to 0.33 wt % carbon before precipitating carbide.

Dyson and Andrews[24] studied the carbides precipitated in alloy steels containing up to 4 wt % chromium and about 0.4 wt % molybdenum by fluorescence analysis and lattice-parameter measurements. They established the composition of carbide as the M_7C_3 type, with an Fe/Cr ratio of about 1/3. The carbide contained very little molybdenum. Furthermore, the composition of the carbide was found to be temperature insensitive in the temperature range 600-700°C. As before, the activity of carbon in equilibrium with the carbide $(Fe,Cr)_7C_3$ with a (Fe/Cr) ratio of 1/3 was computed by using the power relationship for the activity of Cr_7C_3 in the mixed carbide and the free energy of formation[11] of Cr_7C_3:

$$\Delta F^0_{1/3}(Cr_7C_3) = -14000 - 2.0T. \qquad (10)$$

The carbon activities in the alloy at the α-carbide phase boundary thus computed are 0.78 at 700°C, 0.352 at 600°C, and 0.124 at 500°C.

The distribution coefficient for carbon in the ferritic steel-sodium-carbon system was obtained by setting the partial molal free-energy change equal to zero for the reaction

$$\underline{C}(Na) = \underline{C}\ (\text{ferritic alloy});\ \Delta F = \overline{F}_{\underline{C}}(\text{alloy}) - \overline{F}_{\underline{C}}(Na). \tag{11}$$

The results of the calculation are presented in Fig. 16. The ferritic steel commonly used contains only about 0.1 wt % carbon and, if we assume that Henry's law ($a_{\underline{C}} = kN_{\underline{C}}$) is applicable for carbon in the steel, the distribution coefficient may be used to calculate the relation between the carbon concentration in sodium and that in the ferritic steel. This relation and the relation between carbon in an 18-8 stainless steel and that in sodium are shown in Fig. 16.

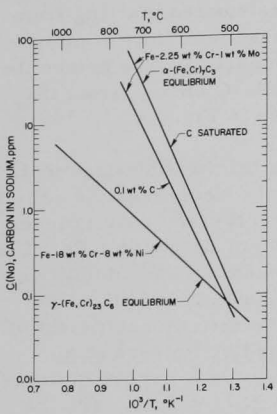

306-462 Rev. 1

Fig. 16. Temperature Dependence of Ferritic Steel and Austenitic Steel--$\underline{C}$(Na)--Carbide Equilibria

It is evident from this figure that the ferritic alloy exposed to sodium containing 1 ppm carbon will not decarburize up to a temperature of about 600°C, while at temperatures above 600°C, decarburization will occur. The driving force for decarburization of the alloy increases with increasing temperature.

It may also be seen from Fig. 16 that, if the 18-8 stainless steel and the ferritic alloy are exposed to sodium free of carbon (i.e., below 0.08 ppm), no carbon transfer is expected from ferritic to austenitic steel below 510°C. At temperatures above 510°C, carbon transfer from the ferritic to austenitic steel will occur under isothermal conditions. A calculation of the carbon activities and solubilities in these alloys shows that isothermal carbon transfer may be completely prevented at 600°C, if the carbon concentration in the ferritic alloy can be reduced to about 240 ppm. However, in an athermal system where the austenitic steel is at a higher temperature, the driving force for carbon transfer diminishes in comparison with that in an isothermal system.

III. KINETIC ASPECTS

The carburization of stainless steel involves the diffusion of carbon in austenite accompanied by carbide precipitation. If stainless steel is exposed to liquid sodium with a carbon activity larger than that in the alloy, then carbon from the sodium diffuses into the alloy and precipitates some fraction of the concentration of elements such as chromium, niobium, or titanium as a dispersed carbide. In the initial stages of precipitation, carbides with high (Cr/Fe) ratios will be precipitated. As the process continues, the carbides in any given region will become richer in iron, and the austenite will become richer in carbon and leaner in chromium. The

process will continue until an equilibrium between the carbide and the austenite is established, and this equilibrium is dependent on the carbon concentration in sodium, as may be seen in Fig. 11. Furthermore, as the total carbon in the precipitated region increases, the volume fraction of carbide to austenite increases; that is, as the process continues, more and more chromium will be present as carbide. As is evident, the assumption that all of the chromium in the precipitated region in the alloy is present as carbide would greatly underestimate the precipitated zone thickness for any given reaction time. For this reason the mathematical models developed in the literature[25-28] for internal oxidation processes are not directly applicable to the carburization of stainless steel. The driving force for carbon diffusion is the difference between the carbon concentration in austenite at the surface of the alloy (established by the carbon concentration in sodium) and the solubility limit for carbon in austenite containing 18 wt % chromium and 8 wt % nickel. Isoactivity lines for carbon may be constructed, as indicated earlier, and the variation of carbon concentration or activity in austenite across the precipitated layer may be computed assuming local equilibrium between the austenite and the carbide.

It is to be mentioned, however, that since diffusion occurs only by virtue of a composition, or more precisely, an activity gradient, any system in which diffusion occurs is not in equilibrium; consequently, reasoning based on an equilibrium diagram alone cannot be strictly valid. We assume, as has been done by others, that equilibrium prevails locally even though the system as a whole is far from equilibrium; in other words, diffusion is slow compared with the rate of reaction to form a new phase. Even with the assumption of local equilibrium between the carbide and the austenite, it is difficult to determine the rate at which the precipitation front advances into the alloy because the carbon concentration profile across the precipitation region for various thicknesses of precipitated zone is not known. Thus, it becomes necessary to conduct experiments to establish these concentration profiles for various precipitation thicknesses and for different carbon concentrations in sodium.

The conditions of temperature in the range of 450 to 800°C and carbon concentrations in sodium between 0.1 and 2 ppm have important implications on the rate and mode of carburization of stainless steel in sodium. For a given carbon concentration in sodium, as the temperature increases the driving force for carburization was shown to decrease while the diffusion coefficient for carbon increases. Since the rate of carburization depends on the product of the driving force and the diffusion coefficient, a maximum in the rate is anticipated at some temperature between 450 and 800°C for a given carbon concentration in the range of 0.1 to 2.0 ppm in sodium. At any temperature the rate will also increase with an increase in carbon concentration in sodium.

IV. EFFECT OF CARBURIZATION ON THE MECHANICAL PROPERTIES OF STAINLESS STEEL

Kirschler and Andrews[29] studied the effect of carburization on the strength properties and ductility of Types 304 and 316 stainless steel exposed to sodium with high carbon activity at 650°C using 60 mil thick specimens. The Type 304 stainless steel was found to have a 4.5 mil carburized layer in 500 hours with carbon penetration into the grain boundaries ahead of the layer. In these alloys the tensile and yield strength increased while the ductility decreased. Similar tests conducted with 15 mil specimens that had been carburized to similar case depths showed greater losses in ductility and increases in strength than were anticipated for the thinner cross sections. Even though these tests showed marked effects on the mechanical properties, the carburization of these alloys in sodium was mainly confined to regions near the surface due to relatively short exposure times. For longer exposures at lower carbon activities in sodium, more representative of the reactor systems, the alloys would be carburized in their entire cross section; and similar, if not greater, effects on the mechanical properties would be anticipated.

Furthermore, at temperatures below about 600°C, the mode of carburization will undergo a transition from carbide precipitation within the grains to predominantly the grain boundary regions. The high diffusion rate at the grain boundary coupled with a large driving force can result in a significant amount of carbide in this region at the lower temperatures even though the total carbon content of the stainless steel will be lower than that indicated by the curves in Fig. 11. The effect of the localized carburization on mechanical properties such as fatigue life and ductility under these conditions has not been established; however, the problem should be considered since the properties may be affected adversely. The problem also becomes important from the standpoint of evaluating the effect of a carbon excursion within reactor systems.

V. CONCLUSIONS

1. An equilibrium relationship was obtained between the total carbon (carbon in austenite + carbon in carbide) in Fe-Cr-Ni alloys and the carbon concentration in sodium at various temperatures. The calculations showed that the Fe-Cr-Ni alloys with nominal initial carbon contents may undergo carburization or decarburization depending upon the carbon concentration in sodium and the temperature in the range 500-800°C. For the same carbon concentration in sodium, the equilibrium total carbon in the alloy increases with a decrease in temperature. Furthermore, at a fixed temperature the total carbon content in the alloy increases with an increase

in the carbon concentration in sodium. Beyond a certain carbon concentration in sodium the type of carbide precipitated will change from $(Cr,Fe)_{23}C_6$ to $(Cr,Fe)_7C_3$. We believe that the carbon content in sodium necessary to yield $(Cr,Fe)_7C_3$ is above that of practical interest in reactor systems.

2. The carbon concentrations in sodium required for incipient carbide precipitation at the various temperatures are well within the solubility limit for carbon in sodium at those temperatures; however, they are significantly lower than values commonly reported for stainless steel-sodium systems (e.g., 15-30 ppm). Recent carbon analyses of the EBR-II primary sodium have yielded values as low as 0.8 ppm.[30] The results in this report suggest that the carbon level in EBR-II sodium is indeed this low and probably is somewhat lower because of the sizeable area of stainless steel in contact with flowing sodium at temperatures of about 500°C.

3. We conclude that, if the carbon concentration in sodium is in equilibrium with Type 304 stainless steel and, if selective mass transfer of chromium occurs, the alloy will tend to decarburize (i.e., chromium and carbon transfer will occur simultaneously from the alloy to sodium). However, if a carbon excursion occurs in a stainless steel-sodium system that has undergone chromium mass transfer, then both the chromium and the total carbon concentrations at the alloy surface are necessary to establish the driving force for carbon diffusion and carbide precipitation.

4. The transfer of carbon from ferritic steel (with 0.1 wt % C) to austenitic stainless steel under isothermal conditions is inevitable at temperatures above 510°C. The driving force for the process increases with an increase in temperature; however, carbon transfer can be reduced by lowering the carbon concentration in the ferritic steel; for example, at 600°C the carbon concentration must be decreased to 240 ppm. In a nonisothermal system where the austenitic steel is at a higher temperature, the driving force for carbon transfer diminishes compared with that in an isothermal system.

5. The reliability of the calculations in this report would be enhanced if the carbon activity values were determined experimentally in Fe-Cr-Ni alloys in the temperature range 500-800°C. The carburizing potentials established by various carbon species in sodium are needed to evaluate their relative importance. For this purpose, better techniques are needed for the analysis of low concentrations (less than 1 ppm) of the different carbon species in sodium. An experimental program in the above areas is in progress. The results should lead to an understanding of the mechanism and kinetics of carbon transport in sodium-steel systems and thus provide a basis for predicting the effect of both carbon excursions and long-term carburization-decarburization processes on the integrity of reactor components.

APPENDIX

The solubility of carbon in Fe-C austenite at different temperatures was obtained from the phase diagram (Fig. 1). The effect of nickel on the activity coefficient of carbon γ_C in Fe-Ni-C austenite in the temperature range 800-1200°C was given by Heckler and Winchell[6] as

$$\ln \gamma_C = 7.5\chi_C + \epsilon_C^{(Ni)}\chi_{Ni}, \tag{12}$$

where

χ_C = mole fraction of carbon in the alloy

χ_{Ni} = mole fraction of nickel in the alloy

$$\epsilon_C^{(Ni)} = \left(\frac{\partial \ln \gamma_C}{\partial \chi_{Ni}}\right)_{T,\chi_C} = 1.3 + 3.5 \times 10^3/T$$

T = temperature, °K.

The interaction parameter $\epsilon_C^{(Ni)}$ was used to compute the difference in the concentration of carbon between γ-Fe and Fe-8 wt % Ni austenite as a function of carbon activity in the austenite at temperatures of 800 and 1000°C. This is shown in Fig. 17. It is evident from this figure that the concentration of carbon in Fe-8 wt % Ni austenite is dependent upon the carbon activity in the alloy.

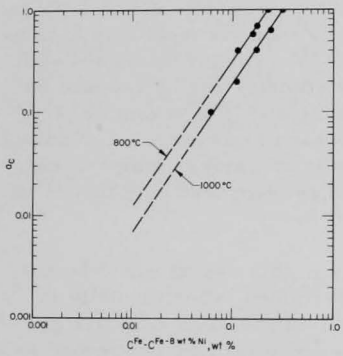

306-597 Rev. 1

Fig. 17

The Difference in the Concentration of Carbon between γ-Fe and Fe-8 wt % Ni Austenite as a Function of Carbon Activity in the Austenite at Temperatures of 800 and 1000°C[6]

The effect of chromium on the Fe-C binary carbon activity at 1000°C was evaluated from the results of Bungardt et al.[4] (see Fig. 3). A plot of the difference in the solubility of carbon in Fe-Cr austenite and the carbon concentration in γ-Fe, per wt % Cr, at isoactivity, for various chromium levels in the Fe-Cr-C alloys, is shown in Fig. 18. To compute the chromium effect at temperatures below 1000°C, a relation between temperature and carbon content of an 18-8 stainless steel proposed by Rocha[7] was used:

$$\ln \chi_C = 1.02 - (7000/T), \tag{13}$$

where

χ_C = mole fraction of carbon in the steel

T = temperature, °K.

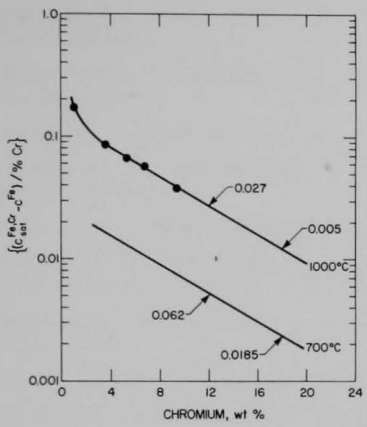

306-452 Rev. 1

Fig. 18

The Difference in the Solubility of Carbon in a Fe-Cr Austenite and the Carbon Concentration in γ-Fe, per wt % Cr, at Isoactivity for Various Chromium Levels in the Fe-Cr-C Alloys. The numbers on the curves indicate carbon activity values at the indicated chromium levels.

Equation 13 yields a carbon solubility value of about 0.045 wt % at 700°C, whereas the carbon activity at 700°C is 0.0185 from Fig. 5. The interaction effect of 18 wt % chromium on carbon in austenite at 700°C was obtained by subtracting from 0.045 wt % the effect of 8 wt % nickel (from Fig. 17). The effect of chromium on the carbon solubility at different chromium levels in the alloy at temperatures of 1000°C and at 700°C was assumed the same and is shown in Fig. 18. The same procedure was used to compute the effect of chromium at lower temperatures.

By using Figs. 1, 17, and 18, the carbon solubility values in Fe-Cr-8 wt % Ni alloys at different temperatures were computed, and are shown in Figs. 6 and 7.

ACKNOWLEDGMENTS

The authors are grateful to Prof. H. W. Paxton of Carnegie-Mellon University for helpful discussions, and also wish to thank P. G. Shewmon, D. L. Smith, J. E. Draley, and F. A. Smith of this Laboratory for their review of this report.

REFERENCES

1. *Metals Handbook*, Lyman, T., Ed., American Society for Metals, 1948, pp. 1182 and 1253.
2. Schenck, H., and Kaiser, H., Arch. Eisenhuttenwes. *31*, 227-235 (1960).
3. Bungardt, K., Kunze, K. E., and Horn, E., Arch. Eisenhuttenwes. *29*, 193-203 (1958).
4. Bungardt, K., Preisendanz, H., and Lehnert, G., Arch. Eisenhuttenwes. *35*, 999-1007 (1964).
5. Stawstrom, C., and Hillert, M., J. Iron Steel Inst. *207*, 77-85 (1969).
6. Heckler, A. J., and Winchell, P. G., Trans. Met. Soc. AIME *227*, 732-736 (1963).
7. Rocha, H. J., DEW - Technische Berichte *2*, 16 (1962).
8. Kassner, T. F., and Smith, D. L., *Calculations on the Kinetics of Oxygen Solution in Ta and Nb in Liquid Sodium Environment*, ANL-7335 (Sept 1967).
9. Longson, B., and Thorley, A. W., *The Solubility of Carbon in Sodium*, to be published.
10. Goldschmidt, H. J., J. Iron Steel Inst. *160*, 345-362 (1948).
11. Richardson, F. D., J. Iron Steel Inst. *175*, 33-51 (1953).
12. Butler, J. F., McCabe, C. L., and Paxton, H. W., Trans. Met. Soc. AIME *221*, 479-484 (1961).
13. Bogers, A. J., and Chirer, E. G., private communication, Nov 1968.
14. Hiltz, R. H., *Effect of Carburization on the Phases of Austenitic Stainless Steel*, Topical Report No. 6, MSAR 66-119 (1966).
15. Anderson, W. J., and Sneesby, G. V., *Carburization of Austenitic Stainless Steel in Liquid Sodium*, NAA-SR-5282 (1960).
16. Valibus, L., Proc. Intl. Conf. on Sodium Technology and Large Fast Reactor Design, ANL-7520, Part I, pp. 93-103 (1968).
17. McCabe, C. L., Hudson, R. G., and Paxton, H. W., Trans. Met. Soc. AIME *212*, 702-705 (1958).
18. Jeannin, Y., Mannerskantz, C., and Richardson, F. D., Trans. Met. Soc. AIME *227*, 300-305 (1963).
19. Furukawa, K., and Nihei, I., Proc. Intl. Conf. on Sodium Technology and Large Fast Reactor Design, ANL-7520, Part I, p. 148 (1968).
20. Roy, P., Wozadlo, G. P., and Comprelli, F. A., Proc. Intl. Conf. on Sodium Technology and Large Fast Reactor Design, ANL-7520, Part I, pp. 131-142 (1968).
21. *Liquid Metals Handbook, Sodium and NaK Supplement*, Foust, O. J. Ed., USAEC, 1967, pp. 3.129-3.131.
22. Smith, R. P., Trans. Met. Soc. AIME *224*, 105-111 (1962).

23. Petrova, E. F., Lapshina, M. I., and Shvartsman, L. A., Metallov *4*, 22-25 (April 1960).

24. Dyson, D. J., and Andrews, K. W., J. Iron Steel Inst. *207*, 208-217 (1969).

25. Rhines, F. N., Johnson, W. A., and Anderson, W. A., Trans. Met. Soc. AIME *147*, 205-221 (1942).

26. Darken, L. S., Trans. Met. Soc. AIME *150*, 157-171 (1942).

27. Wagner, C., Z. Elektrochem. *63*, 772-782 (1959).

28. Swisher, J. H., and Fuchs, E. O., Trans. Met. Soc. AIME *245*, 1789-1794 (1969).

29. Kirschler, L. H., and Andrews, R. C., Proc. Intern. Conf. on Sodium Technology and Large Fast Reactor Design, ANL-7520, Part I, pp. 41-54 (1968).

30. Cissel, D. W., *Reactor Development Program Progress Report, September 1969*, ANL-7618, p. 32 (Oct 1969).